

Extracting cosmological parameters from N-body simulations using machine learning techniques

Andrei Lazanu

Laboratoire de Physique de l'Ecole normale supérieure, ENS, Université PSL, CNRS, Sorbonne Université, Université de Paris, F-75005 Paris, France

E-mail: andrei.lazanu@ens.fr

Abstract. We make use of snapshots taken from the QUIJOTE suite of simulations, consisting of 2000 simulations where five cosmological parameters have been varied (Ω_m , Ω_b , h , n_s and σ_8) in order to investigate the possibility of determining them using machine learning techniques. In particular, we show that convolutional neural networks can be employed to accurately extract Ω_m and σ_8 from the N -body simulations, and that these parameters can also be found from the non-linear matter power spectrum obtained from the same suite of simulations using both random forest regressors and deep neural networks. We show that the power spectrum provides competitive results in terms of accuracy compared to using the simulations and that we can also estimate the scalar spectral index n_s from the power spectrum, at a lower precision.

Contents

1	Introduction	1
2	Numerical simulations and model performance analysis	2
3	Cosmological parameters from the three-dimensional density field	3
4	Cosmological parameters from the power spectrum	4
5	Discussion	7
6	Conclusions and future directions	9

1 Introduction

In recent years, cosmology has increasingly become a precision science and measurements of cosmological observables have achieved an unprecedented level of accuracy. Probes of the Cosmic Microwave Background (CMB), such as COBE, WMAP [1] and *Planck* [2], have been able to measure it with exquisite accuracy and to show that the inflationary paradigm, combined with the growth of primordial quantum fluctuations, provide an excellent agreement with the cosmological data: the six-parameter Λ CDM model [3]. These parameters, together with others that can be derived from them, have been determined increasingly accurately, the current values of the ones used in the *Planck* analysis being: the physical baryon density parameter $\Omega_b h^2 = 0.02242 \pm 0.00014$, the physical dark matter density parameter $\Omega_c h^2 = 0.11933 \pm 0.00091$, the approximation to the acoustic scale angle $100 \theta_{\text{MC}} = 1.04101 \pm 0.00029$, the Thomson scattering optical depth due to reionization $\tau = 0.0561 \pm 0.0071$, the power spectrum of curvature perturbations $\ln(10^{10} A_s) = 3.047 \pm 0.014$, the scalar spectral index $n_s = 0.9665 \pm 0.0038$ (with error bars at 68% confidence level), when considering *Planck* and Baryon Acoustic Oscillations data. Derived parameters include the reduced Hubble constant $h = 67.66 \pm 0.42$, the baryon density parameter $\Omega_b = 0.0486 \pm 0.0010$, the matter density parameter $\Omega_m = 0.3111 \pm 0.0056$ and the amplitude of the root-mean-square matter fluctuation averaged over a sphere of radius at $8h^{-1}$ Mpc, $\sigma_8 = 0.8102 \pm 0.0060$. The CMB represents two-dimensional data from the surface of last scattering, thus providing only a limited number of modes. Moreover, it has already been exploited almost to the limit of cosmic variance. At the same time, the distribution of matter and galaxies – the large scale structure of the Universe (LSS) – contains significantly more modes, due to its three-dimensional nature given by the redshift, in addition to the distribution of galaxies on the sky. The observation of LSS, the modelling and the understanding of its nature are some of the goals of future probes of the large scale structure of the Universe, such as DESI [4], Euclid [5], LSST [6] and SKA [7]. They will be providing in the near future more and more precise measurements of the galaxy distribution. The information encoded in the LSS, complementary to that from the CMB, is however much more difficult to extract, partially due to non-linear mode coupling and its three-dimensional nature. One cannot rely solely on analytical models or perturbative techniques – N -body simulations are generally required, which are usually expensive to run. In parallel, the advances in computational power and processor architecture have allowed the

running of higher and higher resolution numerical simulations, which model the current Universe increasingly realistically. Moreover, this has also allowed storing the outputs of many of these simulations, corresponding to different realisations or to variation of cosmological parameters. Advances in machine learning and data science techniques have allowed the efficient extraction of information from huge datasets. These have become increasingly popular as the amount of information extracted from cosmological surveys has become overwhelming. Machine learning techniques have already been used in a variety of cosmology setups: CMB [8, 9], LSS [10–13], reionization and 21cm [14, 15], gravitational lensing: weak lensing [16, 17], strong lensing [18, 19], redshift prediction [20, 21], parameter estimation [22, 23], and are expected to provide more insights in the future [24]. In particular, such techniques can be applied to observations of the large-scale structure measured from galaxy surveys.

In this work, we use machine learning methods to extract cosmological parameters from numerical simulations and from the non-linear power spectrum as a first step. We leave extensions to galaxy measurements to a future work. The paper is structured as follows: in Section 2 we describe the simulations used in this work, in Section 3 we show how one can extract the input parameters directly from the simulations, in Section 4 we use the non-linear power spectrum to extract the cosmological parameters and in Section 5 we discuss the results.

2 Numerical simulations and model performance analysis

In order to extract the cosmological parameters, we use a subset of 2000 simulations of the QUIJOTE simulations [25], a public suite of 44100 full N -body simulations, ran using the TreePM code Gadget-III [26] in boxes of sides of 1 Gpc/ h . The authors provide a variety of cosmological results in addition to the snapshots of the simulations. In this work, we make use of the three-dimensional density field and the power spectrum measured from the simulations at redshift $z = 0$. The simulations are run starting from $z = 127$ and then evolved in time, where the matter power spectrum and the transfer functions are obtained from CAMB [27] and suitably rescaled. These are used to determine displacements and peculiar velocities using second order perturbation theory, which in turn are used to assign to particles that are initially laid on a regular grid with the 2LPT code [28, 29]. The simulations have a cosmological volume of $1 (h^{-1}\text{Gpc})^3$. The gravitational softening length is set to 1/40 of the mean interparticle distance. The simulations have been run with five parameters using a latin-hypercube sampling, which is a statistical method for generating a near-random sample of parameter values from a multidimensional distribution [30]. The hypercube defining the parameter range is given by: $\Omega_m \in [0.1, 0.5]$, $\Omega_b \in [0.03, 0.07]$, $h \in [0.6, 0.9]$, $n_s \in [0.8, 1.2]$ and $\sigma_8 \in [0.6, 1]$.

After splitting the data into training and test sets, we determine the cosmological parameters using the methods described in the next Sections. We then evaluate the performances of each model, presenting the results in two ways: (i) we plot the predicted value vs the ground truth for the test set; (ii) we determine the relative squared error (RSE) on the test set for each of the parameters in order to quantify the results. The RSE is given by

$$RSE = \frac{\sum_{i=1}^{n_{\text{test}}} (y_{\text{true}}^{(i)} - y_{\text{pred}}^{(i)})^2}{\sum_{i=1}^{n_{\text{test}}} (y_{\text{true}}^{(i)} - \bar{y}_{\text{true}})^2}, \quad (2.1)$$

where n_{test} represents the number of examples in the test set, $y_{\text{true}}^{(i)}$ and $y_{\text{pred}}^{(i)}$ represent the ground truth and predicted value of example i , and \bar{y}_{true} is the average of the ground

truth values of the test set for the parameter in question. In the case of a good parameter determination we expect this quantity to be as close to 0 as possible.

3 Cosmological parameters from the three-dimensional density field

We use the three-dimensional distribution of the density field, interpolated on a 64^3 grid from the standard resolution simulations (512^3 points) to extract the input cosmological parameters. As increasing the grid resolution significantly increases both the memory usage and the execution time, we restrict ourselves to this resolution in this work, and we leave a more comprehensive analysis of the effects of the input size for future work. We note that this interpolation was readily available from the simulations website. We employ a set of 2000 simulations, where the five cosmological parameters have been varied: Ω_m , Ω_b , h , n_s and σ_8 . We are also in possession of the “true” values of the parameters used in the simulations. In order to test the performance of our model, we split the set consisting of 2000 simulations into a training set of 1600 simulations and a test set of 400 simulations.

In order to take advantage of the three-dimensional nature of the data, we employ a deep 3D convolutional network. We start with a convolutional neural network that aims to determine the five cosmological parameters. We have investigated several architectures, with the best one presented schematically in Fig. 1.

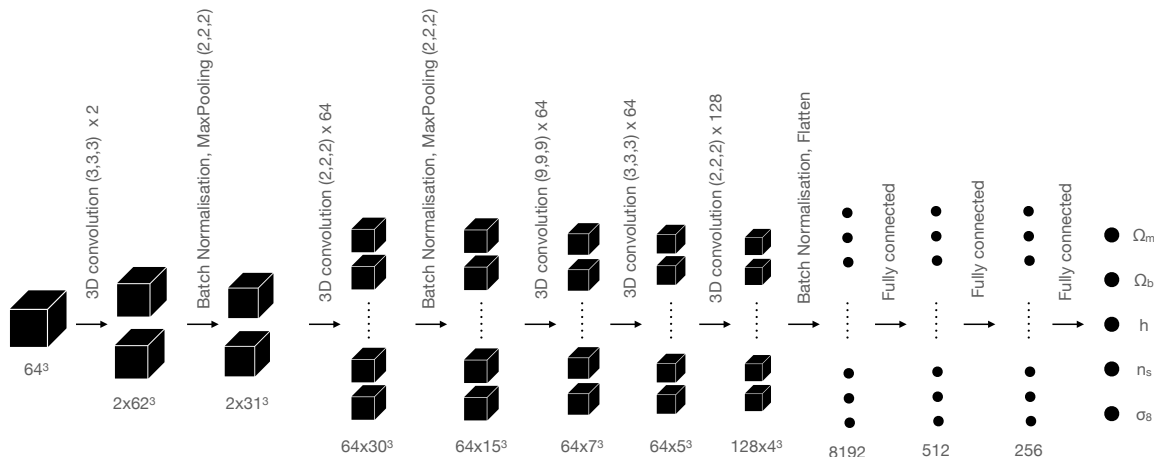


Figure 1. Architecture of the convolutional deep neural network. Starting with a cube of size 64^3 , the network consists of several convolutional layers, followed by Batch Normalisation layers to improve convergence and Max Pooling layers to reduce the space dimensionality. Finally, the network is flattened and contains two fully connected hidden layers, before the five-neuron output corresponding to the original input parameters Ω_m , Ω_b , h , n_s and σ_8 .

The network consists of three types of layers: 3D convolutions, batch normalisation and fully connected layers. We start with a 64^3 -voxel input layer, corresponding to the normalised density field and we consider two 3D convolutions, with a kernel size of $(2, 2, 2)$, followed by a batch normalisation and a max-pooling layer of size $(2, 2, 2)$ to reduce dimensionality. This is followed by 64 $(2, 2, 2)$ convolutions, a batch normalisation layer and a max-pooling layer of size $(2, 2, 2)$. We then add two 3D convolutional layers, of 64 channels and kernel sizes of $(9, 9, 9)$ and $(3, 3, 3)$, followed by a 3D convolutional layer with 128 filters and a kernel

of size $(2, 2, 2)$, followed by batch normalisation and flattening, now getting into a standard deep neural network, where we add two new hidden layers, with 512 and 256 neurons, before the five-neuron output layer, corresponding to the five parameters that have been varied in the simulations. We employ rectified linear unit (ReLU) activation functions throughout the network (defined as $f(x) = \max(0, x)$) and in order to regularise it we have chosen to use two L2 regularisers of size 0.05. We use an Adam optimiser [31] with a learning rate of 5×10^{-5} and default first and second moment exponential decay rates of 0.9 and 0.999 respectively. For the metric, we look at the mean-squared error. We train the network for 50 epochs before it starts overfitting the training set. We have investigated several choices for the regularisation techniques and for the values of its parameters, with the one presented providing the best results. The results on the test set are shown in Fig. 2 for each of the five parameters. We observe that σ_8 is the most accurately predicted, followed by Ω_m , with RSEs of 0.025 and 0.22 respectively. Hence, our analysis shows that, out of the five parameters, the network was able to accurately predict Ω_m and σ_8 , in line with what was found in Ref. [25] from the probability density function. This is most likely due to the weak dependence of the three-dimensional matter overdensity on the other three parameters. We have investigated several architectures before choosing the one presented above. In particular, we have looked at the architecture that was used in Ref. [32], where, apart from the different number of kernels, the authors have used average-pooling layers instead of max-pooling used in our work and a Leaky rectified linear unit [33] instead of the standard ReLU activation. These modifications didn't improve the results in our case.

We therefore concentrate on building a neural network that is able to accurately predict these two parameters. In this case we get to the convergence point after fitting the parameters on the training set for 30 epochs, getting RSEs of 0.23 and 0.015 respectively for Ω_m and σ_8 respectively. We note that the accuracy of the determination of σ_8 is improved, while for Ω_m we obtain a similar result as before. The better accuracy in the prediction of σ_8 using convolutional neural networks confirms the results from Ref. [32], where custom-run simulations have been employed, while another study of such parameter estimation technique can be found in Ref. [34]. As the accuracy of the determination of these two parameters is weaker with respect to that found in [34], we have also investigated the possibility of splitting 128^3 simulations into several 64^3 ones in order to increase the training set size; however, the accuracy of the determination of the parameters was not improved.

4 Cosmological parameters from the power spectrum

In this section, we describe how the power spectrum can be used to extract the cosmological parameters. We note that in Ref. [25] the probability density function has been used to extract the five parameters using a random forest regressor.

The power spectrum $P(k)$ represents the two-point correlation function (in Fourier space) of the matter overdensity,

$$\langle \delta(\mathbf{k})\delta(\mathbf{k}') \rangle = (2\pi)^3 \delta_D(\mathbf{k} + \mathbf{k}') P(k), \quad (4.1)$$

where δ is the matter overdensity and δ_D is the Dirac delta function. In the case of Gaussian fields, the power spectrum contains all the information of the distribution [35]. For three-dimensional large-scale structure probes, the density fields are non-Gaussian on non-linear scales, and therefore contain additional information with respect to the linear power spectrum. Due to their non-linear nature, it is not possible to determine precisely how much of the total information they encode, and how much is stored in higher-order statistics.

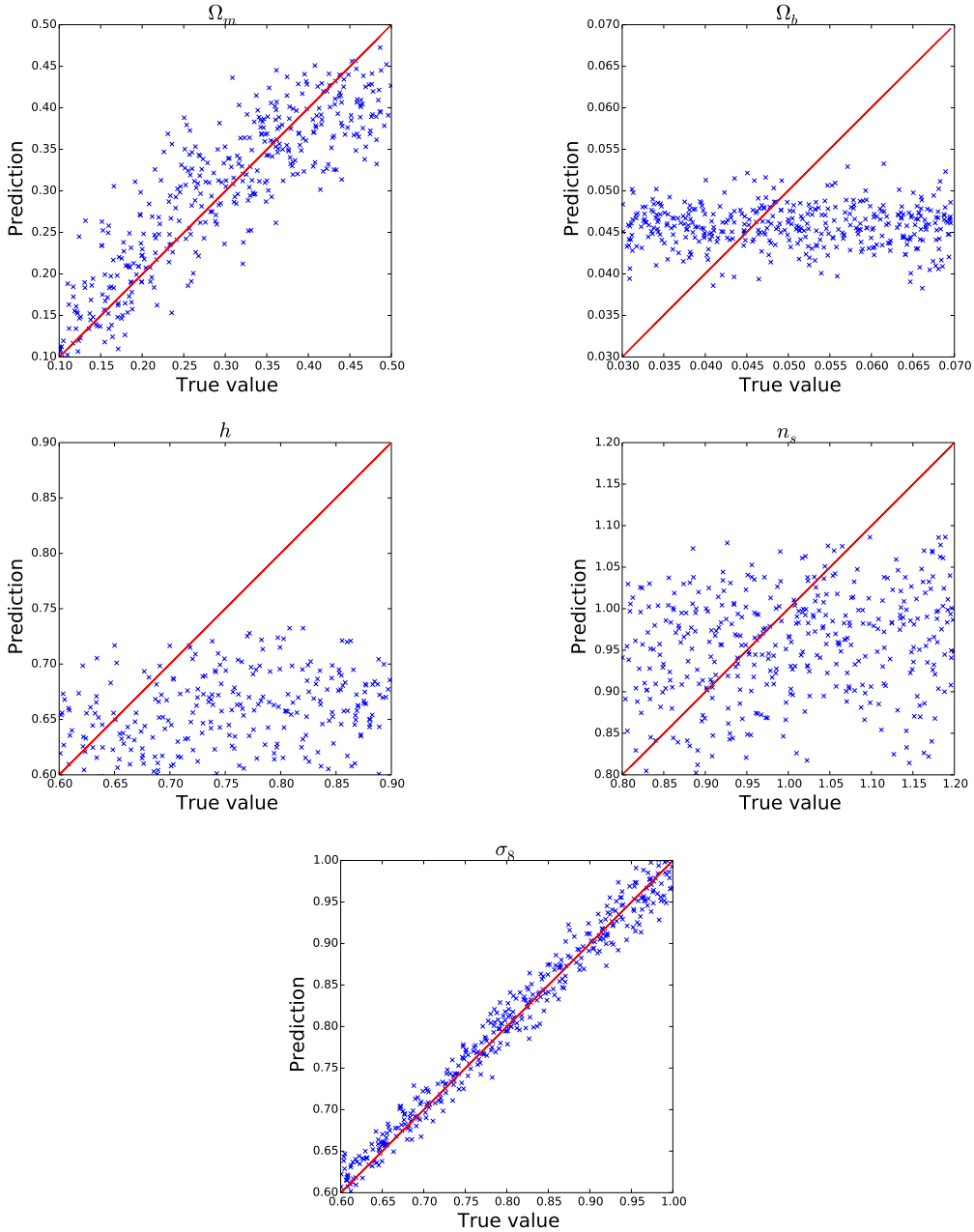


Figure 2. Predictions of Ω_m , Ω_b , h , n_s and σ_8 (right) from the three-dimensional density field extracted from N -body simulations using a convolutional neural network.

Hence, we use the two-point function from the 2000 simulations and we try to extract the five cosmological parameters. As the scale in Fourier space is the same throughout the dataset, we can concentrate only on the column corresponding to the values of the power spectrum. In this case, we use the non-linear power spectrum extracted from the highest resolution QUIJOTE simulations and we use random forest regressors [36] as well as a deep neural network to extract the parameters. In order to improve the precision and the convergence speed of our computations, we take the logarithm of the power spectrum

and in the case of the deep neural network we also normalise it. This preprocessing step is justified by a decrease of the dynamical range of the input variable prior to any normalisation, which makes it more suitable for the use in a machine learning context. We note that σ_8 is determined as an integral over the power spectrum and $n_s \equiv \frac{d \ln P_{\text{lin}}}{d \ln k}$; therefore both can be obtained analytically given the power spectrum. Nevertheless, as these parameters are given as labels to the simulations and to the spectra, we proceed to determine them using random forests and neural networks.

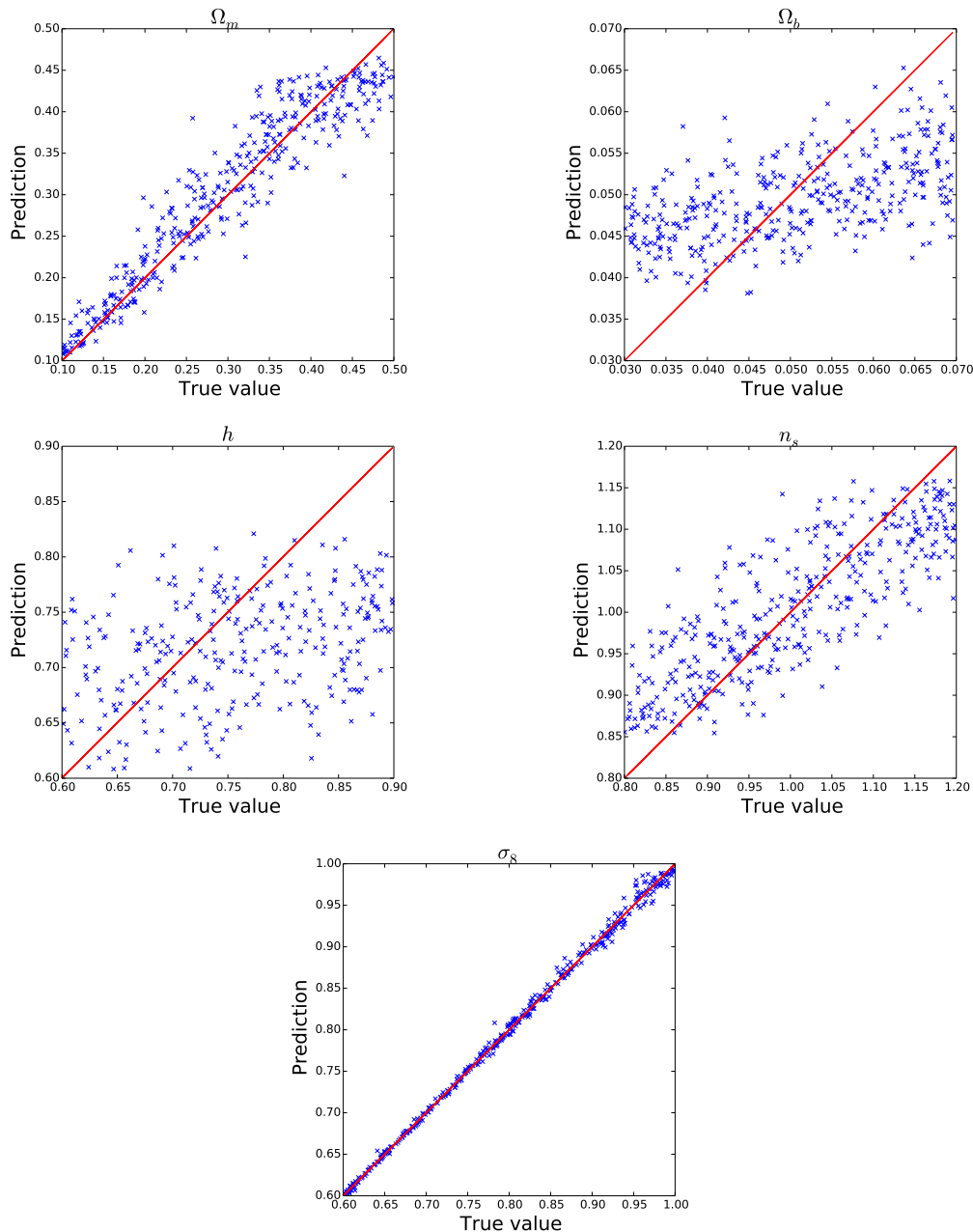


Figure 3. From top to bottom and left to right: Predictions for Ω_m , Ω_b , h , n_s and σ_8 from the non-linear power spectrum extracted from high-resolution simulations using random forest regressors.

In the case of the random forest, the results that we have obtained confirm our findings from the simulations (Fig. 3). The RSEs obtained are at 0.09 for Ω_m , 0.70 for Ω_b , 0.70 for h , 0.33 for n_s and 0.0025 for σ_8 .

As the plots in Fig. 3 show that Ω_b and h are not well determined, we skip these parameters when running our deep neural network. On the other hand, as the error for n_s is significantly reduced, when we employ a deep neural network for the power spectrum, we include Ω_m , n_s and σ_8 . We consider a simple neural network, consisting of three 1024-neurons hidden layers, each followed by a Dropout layer [37], with rates of 0.6 (Fig. 4). The input

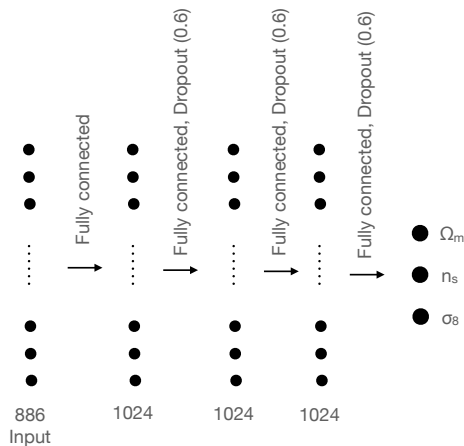


Figure 4. Architecture of the deep neural network used to extract cosmological parameters from the power spectrum. Starting with the values of the spectra in 886 neurons, the network consists of three fully connected dense layers of 1024 neurons, followed Dropout layers where 60% of the data is omitted. Finally, the network ends with the output layer of three neurons corresponding to Ω_m , n_s and σ_8 .

layer has a size of 886 (the number of power spectrum bins), and the output layer has size 3. We are employing an Adam optimizer with a learning rate of 5×10^{-6} [31] and default first and second moment exponential decay rates (0.9 and 0.999). The results that we have obtained are presented in Fig. 5, where the model has been run for 900 epochs, and the RSEs are 0.022 for Ω_m , 0.17 for n_s and 0.0057 for σ_8 .

5 Discussion

In Table 1 we quantify the goodness-of-fit and we present the relative squared errors obtained from the three dimensional density field (via a convolutional neural network) and from the power spectrum (using the random forest regressor and the deep neural network). These results show a significantly better accuracy of the estimation of the parameters involved when using the power spectrum, compared to using the convolutional neural network on the 3D density field. We believe that the lower resolution of the simulations are the cause for the weaker accuracy in determining parameters from the simulations with respect to the power spectrum. In the case of the power spectrum, the inability of the network to

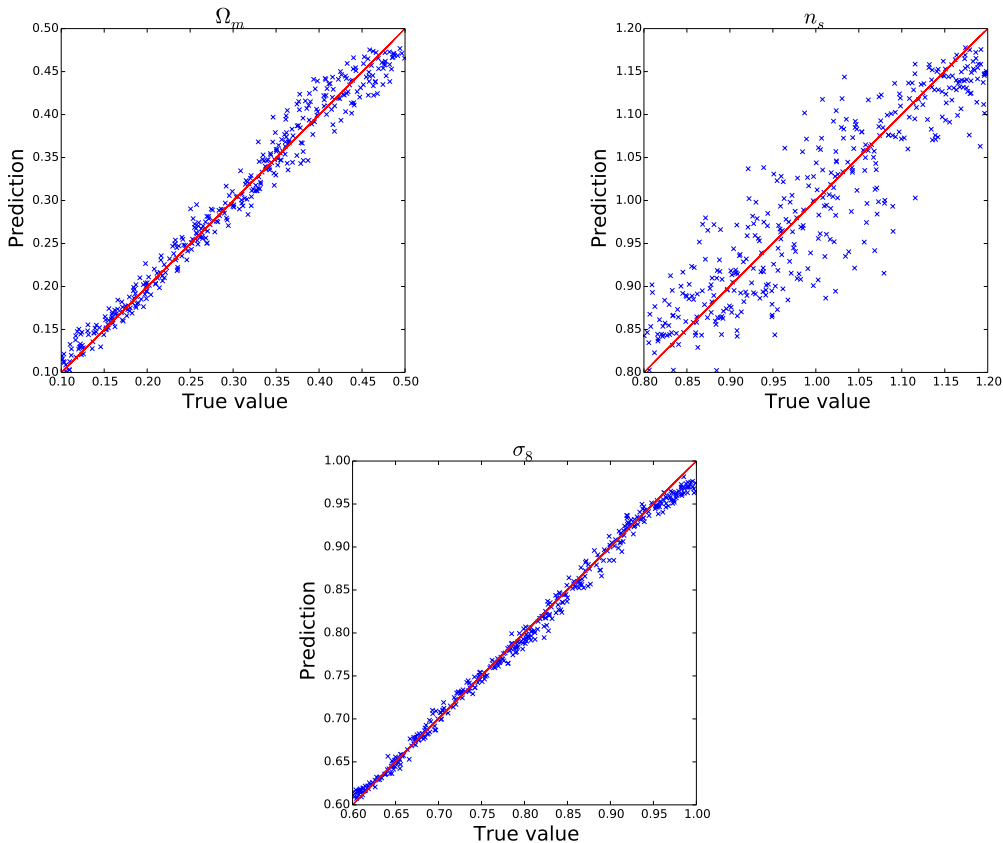


Figure 5. From top to bottom and left to right: Predictions for Ω_m , n_s and σ_8 from the non-linear power spectrum extracted from high-resolution simulations using a deep neural network.

extract Ω_b and h is caused by the degeneracies between them [38]. As σ_8 modifies the global amplitude of the power spectrum, the accurate determination of this parameter was expected. For n_s , which only changes the tilt of the linear power spectrum, we have obtained a much weaker determination, likely due to non-linearities and degeneracies with the other parameters. Finally, increasing Ω_m shifts power into smaller scales, hence providing an observable effect.

Parameter	Simulations (5 parameters)	Simulations (2 parameters)	Power spectrum (RF)	Power spectrum (DNN)
Ω_m	0.22	0.23	0.09	0.022
Ω_b	1.19	–	0.70	–
h	1.35	–	0.70	–
n_s	1.27	–	0.33	0.17
σ_8	0.025	0.015	0.0025	0.0067

Table 1. Relative squared errors on the cosmological parameters obtained from the convolutional neural network using the simulations (left), and from the power spectrum using a random forest regressor (middle) and a deep neural network (right).

6 Conclusions and future directions

In this work, we have shown how information from numerical simulations can be extracted either directly, or after processing, using correlation functions such as the matter power spectrum.

Our results show that, among the parameters that are varied in the QUIJOTE simulations, σ_8 can be extracted with exquisite accuracy, from both simulations (through the 3D density field) and the power spectrum. The matter fraction Ω_m can also be extracted from both the simulations and the power spectrum, although less accurately. We also show that the spectral index can be determined from the power spectrum using a deep neural network. Of course, the information stored in the non-linear power spectrum also appears in the density field, and therefore we conclude that the low resolution (64^3) does not capture all the relevant information from the simulation. As the training time and the memory requirements of increasing the input size from 64^3 points to 128^3 or 256^3 for each example and using them directly would be significantly increased and a very different network configuration is likely to be required, we leave such a study for future work, where we plan to investigate the optimal methods of extracting the cosmological parameters using convolutional neural networks.

These type of methods could be eventually used to determine the parameters from measured galaxy patterns on the sky. The methods would require further refining as in this work we have only focused on the matter distribution. A study of the bias between the dark matter and galaxy distributions would also be required.

Acknowledgments

AL acknowledges funding by the LabEx ENS-ICFP: ANR-10-LABX-0010/ANR-10-IDEX-0001-02 PSL*.

References

- [1] C. L. Bennett, M. Bay, M. Halpern, G. Hinshaw, C. Jackson, N. Jarosik et al., *The Microwave Anisotropy Probe Mission*, *Astrophys. J.* **583** (Jan., 2003) 1–23, [[astro-ph/0301158](#)].
- [2] PLANCK collaboration, N. Aghanim et al., *Planck 2018 results. I. Overview and the cosmological legacy of Planck*, *Astron. Astrophys.* **641** (2020) A1, [[1807.06205](#)].
- [3] S. Weinberg, *The cosmological constant problem*, *Rev. Mod. Phys.* **61** (Jan, 1989) 1–23.
- [4] DESI collaboration, M. Levi et al., *The DESI Experiment, a whitepaper for Snowmass 2013*, [1308.0847](#).
- [5] EUCLID collaboration, R. Laureijs et al., *Euclid Definition Study Report*, [1110.3193](#).
- [6] LSST SCIENCE, LSST PROJECT collaboration, P. A. Abell et al., *LSST Science Book, Version 2.0*, [0912.0201](#).
- [7] M. J. Jarvis, D. Bacon, C. Blake, M. L. Brown, S. N. Lindsay, A. Raccanelli et al., *Cosmology with SKA Radio Continuum Surveys*, [1501.03825](#).
- [8] J. a. Caldeira, W. L. K. Wu, B. Nord, C. Avestruz, S. Trivedi and K. T. Story, *DeepCMB: Lensing Reconstruction of the Cosmic Microwave Background with Deep Neural Networks*, *Astron. Comput.* **28** (2019) 100307, [[1810.01483](#)].
- [9] P. Chanda and R. Saha, *An Unbiased Estimator of the Full-sky CMB Angular Power Spectrum using Neural Networks*, [2102.04327](#).

- [10] A. C. Rodriguez, T. Kacprzak, A. Lucchi, A. Amara, R. Sgier, J. Fluri et al., *Fast cosmic web simulations with generative adversarial networks*, *Comput. Astrophys. Cosmol.* **5** (2018) 4, [[1801.09070](#)].
- [11] L. Lucie-Smith, H. V. Peiris, A. Pontzen, B. Nord and J. Thiyagalingam, *Deep learning insights into cosmological structure formation*, [2011.10577](#).
- [12] Z. Lin, N. Huang, C. Avestruz, W. L. K. Wu, S. Trivedi, J. Caldeira et al., *DeepSZ: Identification of Sunyaev-Zel'dovich Galaxy Clusters using Deep Learning*, [2102.13123](#).
- [13] X. Xu, S. Kumar, I. Zehavi and S. Contreras, *Predicting halo occupation and galaxy assembly bias with machine learning*, [2107.01223](#).
- [14] H. Shimabukuro and B. Semelin, *Analysing the 21 cm signal from the epoch of reionization with artificial neural networks*, *Mon. Not. Roy. Astron. Soc.* **468** (2017) 3869–3877, [[1701.07026](#)].
- [15] L. Huang, R. A. C. Croft and H. Arora, *Deep Forest: Neural Network reconstruction of the Lyman-alpha forest*, [2009.10673](#).
- [16] D. Ribli, B. A. Pataki and I. Csabai, *An improved cosmological parameter inference scheme motivated by deep learning*, *Nature Astron.* **3** (2019) 93–98, [[1806.05995](#)].
- [17] J. M. Zorrilla Matilla, M. Sharma, D. Hsu and Z. Haiman, *Interpreting deep learning models for weak lensing*, *Phys. Rev. D* **102** (2020) 123506, [[2007.06529](#)].
- [18] C. Jacobs, K. Glazebrook, T. Collett, A. More and C. McCarthy, *Finding strong lenses in CFHTLS using convolutional neural networks*, *Mon. Not. Roy. Astron. Soc.* **471** (2017) 167–181, [[1704.02744](#)].
- [19] LSST DARK ENERGY SCIENCE collaboration, J. W. Park, S. Wagner-Carena, S. Birrer, P. J. Marshall, J. Y.-Y. Lin and A. Roodman, *Large-Scale Gravitational Lens Modeling with Bayesian Neural Networks for Accurate and Precise Inference of the Hubble Constant*, *Astrophys. J.* **910** (2021) 39, [[2012.00042](#)].
- [20] A. A. Collister and O. Lahav, *ANNz: Estimating photometric redshifts using artificial neural networks*, *Publ. Astron. Soc. Pac.* **116** (2004) 345–351, [[astro-ph/0311058](#)].
- [21] M. Eriksen et al., *The PAU Survey: Photometric redshifts using transfer learning from simulations*, *Mon. Not. Roy. Astron. Soc.* **497** (2020) 4565–4579, [[2004.07979](#)].
- [22] J. Alsing, T. Charnock, S. Feeney and B. Wandelt, *Fast likelihood-free cosmology with neural density estimators and active learning*, *Mon. Not. Roy. Astron. Soc.* **488** (2019) 4440–4458, [[1903.00007](#)].
- [23] A. Kostić, J. Jasche, D. K. Ramanah and G. Lavaux, *Machine-driven searches for cosmological physics*, [2107.00657](#).
- [24] M. Ntampaka et al., *The Role of Machine Learning in the Next Decade of Cosmology*, [1902.10159](#).
- [25] F. Villaescusa-Navarro, C. Hahn, E. Massara, A. Banerjee, A. M. Delgado, D. K. Ramanah et al., *The Quijote Simulations*, *Astrophys. J. Supp.* **250** (Sept., 2020) 2, [[1909.05273](#)].
- [26] V. Springel, *The Cosmological simulation code GADGET-2*, *Mon. Not. Roy. Astron. Soc.* **364** (2005) 1105–1134, [[astro-ph/0505010](#)].
- [27] A. Lewis, A. Challinor and A. Lasenby, *Efficient computation of CMB anisotropies in closed FRW models*, *Astrophys. J.* **538** (2000) 473–476, [[astro-ph/9911177](#)].
- [28] R. Scoccimarro, *Transients from initial conditions: a perturbative analysis*, *Mon. Not. Roy. Astron. Soc.* **299** (1998) 1097, [[astro-ph/9711187](#)].
- [29] M. Crocce, S. Pueblas and R. Scoccimarro, *Transients from Initial Conditions in Cosmological Simulations*, *Mon. Not. Roy. Astron. Soc.* **373** (2006) 369–381, [[astro-ph/0606505](#)].

- [30] M. D. McKay, R. J. Beckman and W. J. Conover, *A comparison of three methods for selecting values of input variables in the analysis of output from a computer code*, *Technometrics* **21** (1979) 239–245.
- [31] D. P. Kingma and J. Ba, *Adam: A Method for Stochastic Optimization*, [1412.6980](#).
- [32] S. Ravanbakhsh, J. Oliva, S. Fromenteau, L. C. Price, S. Ho, J. Schneider et al., *Estimating Cosmological Parameters from the Dark Matter Distribution*, [1711.02033](#).
- [33] A. L. Maas, A. Y. Hannun and A. Y. Ng, *Rectifier nonlinearities improve neural network acoustic models*, in *in ICML Workshop on Deep Learning for Audio, Speech and Language Processing*, 2013.
- [34] S. Pan, M. Liu, J. Forero-Romero, C. G. Sabiu, Z. Li, H. Miao et al., *Cosmological parameter estimation from large-scale structure deep learning*, *Sci. China Phys. Mech. Astron.* **63** (2020) 110412, [[1908.10590](#)].
- [35] L. Verde, *A practical guide to Basic Statistical Techniques for Data Analysis in Cosmology*, [0712.3028](#).
- [36] L. Breiman, *Random forests*, *Machine Learning* **45** (2001) 5–32.
- [37] N. Srivastava, G. Hinton, A. Krizhevsky, I. Sutskever and R. Salakhutdinov, *Dropout: A simple way to prevent neural networks from overfitting*, *Journal of Machine Learning Research* **15** (2014) 1929–1958.
- [38] S. Brieden, H. Gil-Marín and L. Verde, *ShapeFit: Extracting the power spectrum shape information in galaxy surveys beyond BAO and RSD*, [2106.07641](#).